Acta Crystallographica Section F
Structural Biology and Crystallization Communications
ISSN 1744-3091

Crystallization and preliminary X-ray crystallographic analysis of bacterial tRNA^{Sec} in complex with seryl-tRNA synthetase

Yuzuru Itoh,[a,b,c] Shun-ichi Sekine[a,b] and Shigeyuki Yokoyama[a,b]*

[a]Department of Biophysics and Biochemistry, Graduate School of Science, The University of Tokyo, 7-3-1 Hongo, Bunkyo-ku, Tokyo 113-0033, Japan, [b]RIKEN Systems and Structural Biology Center, 1-7-22 Suehiro, Tsurumi, Yokohama 230-0045, Japan, and [c]Laboratory of Membrane and Cytoskeleton Dynamics, Institute of Molecular and Cellular Biosciences, The University of Tokyo, 1-1-1 Yayoi, Bunkyo-ku, Tokyo 113-0032, Japan

Correspondence e-mail: yokoyama@biochem.s.u-tokyo.ac.jp

Received 7 March 2012
Accepted 12 April 2012

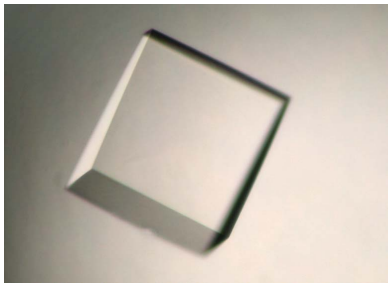

Selenocysteine (Sec) is translationally incorporated into proteins in response to the UGA codon. The tRNA specific to Sec (tRNA^{Sec}) is first ligated with serine by seryl-tRNA synthetase (SerRS). To elucidate the tertiary structure of bacterial tRNA^{Sec} and its specific interaction with SerRS, the bacterial tRNA^{Sec} from *Aquifex aeolicus* was crystallized as the heterologous complex with the archaeal SerRS from *Methanopyrus kandleri*. Although X-ray diffraction by crystals of tRNA^{Sec} in complex with wild-type SerRS was rather poor (to 5.7 Å resolution), the resolution was improved by introducing point mutations targeting the crystal-packing interface. Heavy-atom labelling also contributed to resolution improvement. A 3.2 Å resolution diffraction data set for phase determination was obtained from a $K_2Pt(CN)_4$-soaked crystal.

1. Introduction

Selenocysteine (Sec), the 21st amino acid, contains selenium and is translationally incorporated into proteins (Böck *et al.*, 1991). The Sec-specific tRNA (tRNA^{Sec}) is the longest tRNA and contains an anticodon complementary to the stop codon UGA (Leinfelder *et al.*, 1988). The secondary structures of tRNA^{Sec} species from bacteria and eukarya/archaea are quite different from the canonical structure and even from each other (Sturchler *et al.*, 1993; Baron *et al.*, 1993; Jühling *et al.*, 2009). In contrast to the canonical amino acids, Sec is synthesized on tRNA^{Sec} through multiple steps, in which tRNA^{Sec} is first ligated with serine by seryl-tRNA synthetase (SerRS; Leinfelder *et al.*, 1988) and serine is then converted to Sec. SerRS is also responsible for serine ligation to the canonical tRNA^{Ser}, which has been analyzed using crystal structures of the SerRS–tRNA^{Ser} complex (Biou *et al.*, 1994).

Although crystal structures of eukaryal and archaeal tRNA^{Sec} species have been reported (Itoh *et al.*, 2009; Chiba *et al.*, 2010), that of bacterial tRNA^{Sec} has not been solved. Furthermore, structural information on the SerRS–tRNA^{Sec} complex is required in order to understand the tRNA-specificity mechanism of SerRS, which recognizes distinct tRNA species. In this communication, we report the crystallization of the bacterial tRNA^{Sec} from *Aquifex aeolicus* in complex with the heterologous SerRS from the archaeon *Methanopyrus kandleri*. Strategies for improvement of diffraction resolution and phase determination are also discussed.

2. Materials and methods

2.1. Overexpression and purification of *M. kandleri* SerRS

The *M. kandleri* SerRS gene was cloned into pET26b vector (Novagen). Point mutations were introduced with a QuikChange site-directed mutagenesis kit (Stratagene). *Escherichia coli* strain Rosetta 2 (DE3) (Stratagene) was transformed with the expression plasmids and the proteins were overexpressed in LB medium at 310 K. The selenomethionine-substituted SerRS mutant was overexpressed in *E. coli* Rosetta 2 (DE3) transformed with the same vector as that encoding the native protein. The cells were grown in M9 minimal medium at 310 K to an OD_{600} of 0.25; 60 mg l^{-1} L-selenomethionine (SeMet), 100 mg l^{-1} each of L-threonine, L-lysine and L-phenylalanine and 50 mg l^{-1} each of L-leucine, L-isoleucine and L-valine

were then added to the medium. After a 15 min pre-incubation, gene expression was induced by adding 0.2 m*M* isopropyl *β*-D-1-thio-galactopyranoside. The cells were cultured at 298 K for a further 22 h prior to harvesting.

The harvested cells expressing wild-type and mutant SerRSs were resuspended in 50 m*M* Tris–HCl buffer pH 8.5 containing 500 m*M* NaCl, 500 m*M* $MgCl_2$, 10 m*M* *β*-mercaptoethanol (*β*-ME) and were disrupted using an ultrasonic homogenizer. The supernatant of the lysate was incubated at 358 K for 30 min to denature and remove most of the *E. coli* proteins. After centrifugation, ammonium sulfate was added to the supernatant (final concentration 2 *M*), which was applied onto a Toyopearl Phenyl-650 column (Tosoh). The column was washed with 20 m*M* Tris–HCl buffer pH 7.5 containing 2.0 *M* ammonium sulfate and 10 m*M* *β*-ME and the proteins were eluted with a linear gradient of 2.0–0 *M* ammonium sulfate. They were dialyzed against 20 m*M* Tris–HCl buffer pH 7.5 containing 0.2–0.4 *M* NaCl and 10 m*M* *β*-ME and concentrated to 12–15 mg ml^{-1}.

2.2. Lysine methylation

Methylation of the lysine residues in wild-type and mutant SerRS was performed using formaldehyde and dimethylamine–borane complex as described by Walter *et al.* (2006). Prior to methylation, the proteins were diluted with 20 m*M* HEPES–NaOH buffer pH 7.5 containing 0.4–0.8 *M* NaCl and 10 m*M* *β*-ME. The methylation reagents were removed by repeated dialyses against Tris–HCl buffer pH 7.5 containing 0.2–0.4 *M* NaCl and 10 m*M* *β*-ME.

2.3. Preparation of the tRNA transcript

The gene encoding *A. aeolicus* $tRNA^{Sec}$ was cloned into the pUC119 vector together with the T7 promoter sequence. The template DNA for *in vitro* transcription was amplified by PCR using the plasmid as the template. In the PCR reaction, the M13 forward primer and the primer complementary to the 3′ end of the target tRNA were used. The tRNA was transcribed *in vitro* with T7 RNA polymerase, as described previously (Sekine *et al.*, 1996), and was purified by chromatography on a Resource Q column (GE Healthcare). The purified tRNA was dissolved in 10 m*M* Tris–HCl buffer pH 8.0 containing 10 m*M* $MgCl_2$ and was heated to 338 K for 5 min for refolding.

2.4. Crystallization and diffraction data collection

The complex of wild-type *M. kandleri* SerRS and *A. aeolicus* $tRNA^{Sec}$ was prepared by mixing the components at final concentrations of 80 and 120 µ*M*, respectively, in 20 m*M* Tris–HCl buffer pH 7.5 containing NaCl (100 m*M* for wild-type SerRS and 400 m*M* for the mutants), 10 m*M* $MgCl_2$, 3 m*M* *β*-ME, 500 µ*M* 5′-*O*-[*N*-(L-seryl)sulfamoyl]adenosine (Ser-SA). Ser-SA is a nonhydrolyzable analogue of seryl-adenylate.

Crystallization was performed at 293 K using the sitting-drop vapour-diffusion method by mixing the SerRS–$tRNA^{Sec}$ solution and reservoir solution in a 1:1 ratio. Four screening kits, Crystal Screen 2, Natrix (Hampton Research) and Wizard I and II (Emerald BioSystems), were used for initial screening of the crystallization conditions. The initial crystallization conditions were refined by optimizing the reservoir-solution composition, including the precipitant concentration, buffer pH and additives.

Prior to the X-ray diffraction experiment, the crystals were transferred into a cryoprotective solution and flash-cooled in a cryocooled N_2 stream (∼90 K). For all experiments, an optimized cryoprotective solution (100 m*M* trisodium citrate–HCl buffer pH 5.6 containing 2.0 *M* ammonium sulfate, 1.7 *M* lithium sulfate, 75 m*M* potassium sodium tartrate and 10 m*M* $MgCl_2$) was used. Diffraction data were collected under a cryocooled N_2 stream on BL41XU at SPring-8 (Hyogo, Japan), and BL5A, NE3A and NW12A at the

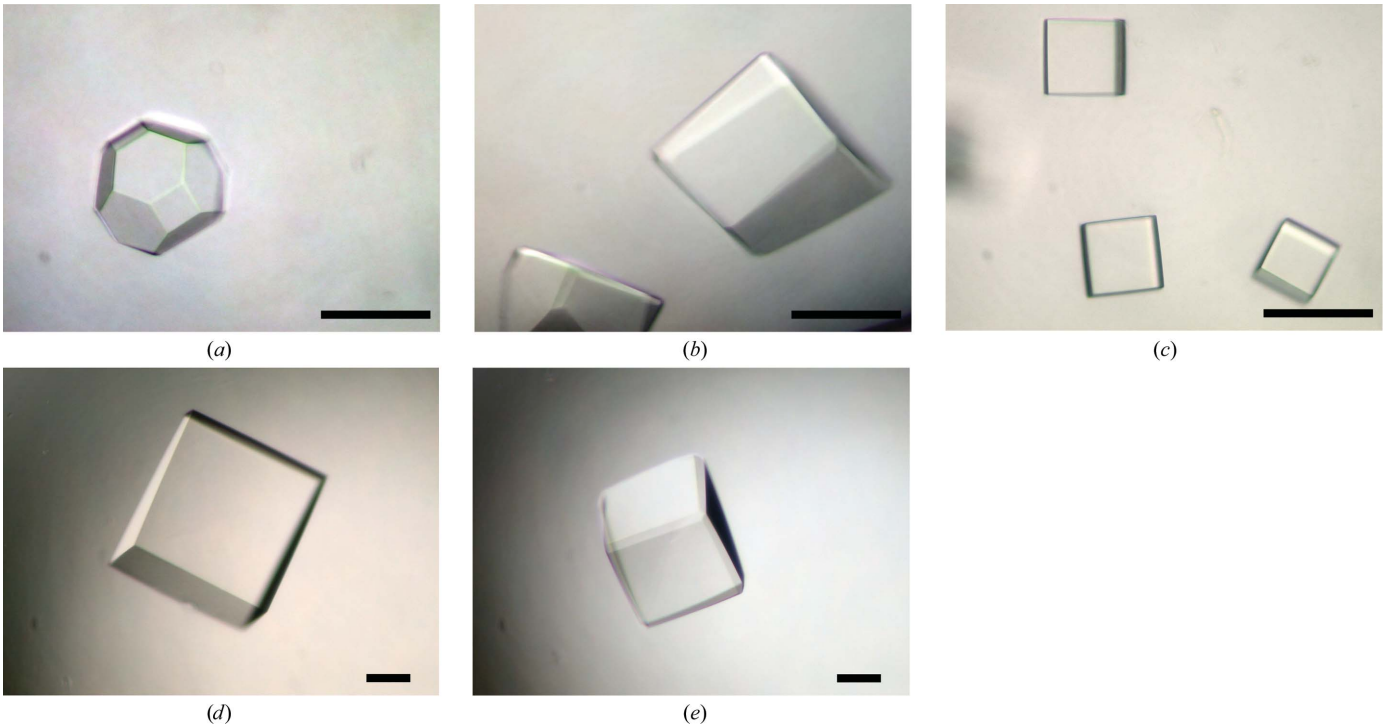

Figure 1
Crystals of the *M. kandleri* SerRS–*A. aeolicus* $tRNA^{Sec}$ complex. Typical crystals of the $tRNA^{Sec}$ in complex with the wild-type SerRS (*a*), Lys-methylated wild-type SerRS (*b*), Lys-methylated $SerRS^{Set2}$ (*c*), Lys-methylated native $SerRS^{Set3}$ (*d*) and Lys-methylated $SerRS^{Set3}$ with SeMet substitution (*e*) are shown. Each scale bar indicates 200 µm.

Table 1
Data-collection and phasing statistics.

Values in parentheses are for the highest resolution shell. FOM, figure of merit; DM, density modification (solvent flattening).

SerRS mutation	Wild type	Wild type	Wild type	Set2	Set2	Set3	Set3			Set3 [SeMet]
Lys methylation	−	−	+	+	+	+	+			+
Heavy-atom labelling		$HgCl_2$			$HgCl_2$		$K_2Pt(CN)_4$			$K_2Pt(CN)_4$
Data collection										
Beamline	SPring-8 BL41XU	SPring-8 BL41XU	SPring-8 BL41XU	SPring-8 BL41XU	PF NW12A	PF BL5A	PF NE3A			PF BL5A
Wavelength (Å)	0.97917	1.00000	1.00000	0.97896	1.00418 [peak]	1.00000	1.07186 [peak]	1.07227 [edge]	1.05404 [remote]	0.97848
Space group	*I*432	*I*432	*P*432	*I*432	*I*432	*I*432	*I*432			*I*432
Unit-cell parameters (Å)	$a = b = c =$ 269.8	$a = b = c =$ 273.2	$a = b = c =$ 271.6	$a = b = c =$ 274.4	$a = b = c =$ 274.7	$a = b = c =$ 274.0	$a = b = c =$ 273.1			$a = b = c =$ 272.8
Resolution (Å)	50.0–5.70 (5.90–5.70)	50.0–6.30 (6.52–6.30)	50.0–6.10 (5.32–6.10)	50.0–4.60 (4.76–4.60)	50.0–4.70 (4.87–4.70)	50.0–3.95 (4.09–3.95)	50.0–3.20 (3.31–3.20)	50.0–3.20 (3.31–3.20)	50.0–3.20 (3.31–3.20)	50.0–3.10 (3.21–3.10)
Unique reflections	5141 (482)	3978 (372)	8667 (837)	10021 (980)	9491 (933)	15660 (1545)	28852 (2825)	28815 (2835)	27446 (2694)	31714 (3126)
Completeness (%)	99.6 (99.8)	99.9 (100.0)	100.0 (99.8)	99.7 (100.0)	100.0 (100.0)	99.8 (100.0)	99.9 (100.0)	99.9 (100.0)	99.9 (100.0)	99.9 (100.0)
Mutliplicity	13.3 (12.4)	20.6 (21.1)	17.3 (12.4)	14.2 (13.9)	20.8 (21.0)	19.6 (19.3)	21.6 (21.7)	21.3 (19.4)	21.0 (18.4)	14.6 (15.0)
R_{merge}†	0.087 (>1)	0.098 (>1)	0.104 (>1)	0.153 (>1)	0.138 (>1)	0.083 (>1)	0.101 (>1)	0.091 (>1)	0.098 (>1)	0.094 (0.847)
$\langle I/\sigma(I)\rangle$	25.1 (2.14)	30.4 (2.19)	24.5 (2.13)	14.5 (2.06)	21.3 (2.16)	31.8 (2.01)	34.7 (2.78)	33.6 (2.20)	31.5 (1.77)	28.4 (3.49)
Phasing		SIRAS [Hg]			SIRAS [Hg]		MAD [Pt]			
No. of identified heavy-atom sites		0.5‡			0.5‡		11			
Phasing power										
Iso (acentric/centric)		0.760/0.463			0.788/0.522		—	0.917/0.819	0.537/0.471	
Ano		0.605			0.216		2.20	1.42	1.36	
FOM (before DM/ after DM)		0.260/0.325			0.231/0.680		0.460/0.811			

† $R_{merge} = \sum_{hkl}\sum_i |I_i(hkl) - \langle I(hkl)\rangle| / \sum_{hkl}\sum_i I_i(hkl)$, where $I_i(hkl)$ is the intensity of the ith measurement of reflection hkl and $\langle I(hkl)\rangle$ is the average value of $I_i(hkl)$ for all i measurements. ‡ Special position.

Photon Factory (PF; Tsukuba, Japan). The data were processed with *HKL*-2000 (Otwinowski & Minor, 1997).

2.5. Soaking of the heavy-atom reagent

The crystals were washed with the reservoir solution and then transferred into a solution of the heavy-atom reagent diluted in the reservoir solution. After 10–15 h incubation, the crystals were transferred into the cryoprotective solution and flash-cooled. The X-ray absorption fine structure (XAFS) was measured to monitor the heavy-atom labelling and to estimate the peak and edge wavelengths of the anomalous scattering.

2.6. Phase determination

Phaser (McCoy *et al.*, 2007) was used for molecular replacement and *autoSHARP* (Vonrhein *et al.*, 2007) was used for phase calculation by the single isomorphous replacement with anomalous scattering (SIRAS) and multiwavelength anomalous dispersion (MAD) methods. *DM* (Winn *et al.*, 2011) was used for subsequent density modification.

3. Results

3.1. Crystallization and diffraction analysis of the SerRS–tRNA^{Sec} complex with wild-type SerRS

Initial crystallization-condition screening of the complex of *M. kandleri* SerRS and *A. aeolicus* tRNA^{Sec} yielded cube-shaped crystals using reservoir solution No. 14 of Crystal Screen 2 (100 m*M* trisodium citrate–HCl buffer pH 5.6 containing 2.0 *M* ammonium sulfate and 200 m*M* potassium sodium tartrate). A brief optimization trial of the reservoir solution indicated that the initial conditions were the best. An ∼250 µm crystal obtained by mixing 0.75 µl complex solution and 0.75 µl reservoir solution (Fig. 1*a*) diffracted to 5.7 Å resolution. The crystal belonged to space group *I*432, with unit-cell parameters $a = b = c = 270$ Å (Table 1).

In order to improve the diffraction resolution, methylation of the lysine residues of SerRS was examined. The complex with Lys-methylated SerRS was crystallized under the same conditions as used for SerRS without Lys methylation and somewhat larger crystals were obtained (Fig. 1*b*). An ∼400 µm crystal diffracted to 6.1 Å resolution and belonged to space group *P*432, with unit-cell parameters $a = b = c = 272$ Å (Table 1). Although the crystallization efficiency was improved, the diffraction resolution was rather worse and was accompanied by a slight expansion of the unit-cell length.

3.2. Preliminary phasing of the wild-type SerRS–tRNA^{Sec} complex

Point mutations targeting the protein surface that participates in crystal packing are expected to improve the diffraction resolution. To estimate the crystal-packing surface, various positions within SerRS and tRNA^{Sec} were investigated using the molecular-replacement method. *M. kandleri* SerRS consists of an N-terminal tRNA-binding domain (residues 1–167) and a C-terminal catalytic domain (residues 168–527). The position of the C-terminal domain was identified by using the corresponding domain structure from the structure of *Methanosarcina barkeri* SerRS (PDB entry 2cj9; Bilokapic *et al.*, 2006) as the search model. The asymmetric unit contained one subunit of the SerRS homodimer, which was built by the crystallographic symmetry. In contrast, the N-terminal domain of SerRS and tRNA^{Sec} were not found.

The SIRAS method was employed to estimate the positions of the N-terminal domain of SerRS and tRNA^{Sec}. A mercury-labelled SerRS–tRNA^{Sec} complex was obtained by cocrystallization in 5.0 m*M* $HgCl_2$ diluted with the reservoir solution (100 m*M* trisodium citrate–HCl buffer pH 5.6 containing 2.1 *M* ammonium sulfate and 200 m*M* potassium sodium tartrate). The mercury-labelled crystal (∼150 µm in size) was transferred into the cryoprotective solution and diffraction data were collected. The crystal diffracted to a resolution of 6.3 Å and belonged to space group *I*432, with unit-cell parameters $a = b = c = 273$ Å (Table 1). A 0.5 site (special position) for the Hg atom was identified based on peaks in the $|F_{\text{Hg-derivative}}| - |F_{\text{native}}|$ map

and the anomalous-difference Fourier map generated using the initial phase calculated by the molecular-replacement method. The experimental phase was calculated using the identified mercury site (Table 1). The $|F_o|$ map generated by the experimental phase indicated the rough electron density of the components.

3.3. Improvement by point mutations (first trial)

The $|F_o|$ map indicated that the N-terminal domain of SerRS participates in protein–protein contacts in the crystal packing, in contrast to the C-terminal domain. To reinforce the crystal packing, Tyr residues were introduced into the contact surface. Four point mutations K100Y/R103Y/D126Y/D127Y (SerRS^{Set1}) and five point mutations R55Y/E58Y/E62Y/R116Y/D118Y (SerRS^{Set2}) were introduced into SerRS and crystallization of the SerRS–tRNA^{Sec} complexes was attempted. No crystals were obtained when the SerRS^{Set1} mutant (with or without Lys methylation) was used. In contrast, the complex of the SerRS^{Set2} mutant (SerRS^{Set2}–tRNA^{Sec} complex) crystallized, although crystal growth was quite slow. The growth rate was somewhat enhanced by using Lys-methylated SerRS^{Set2} and a reservoir solution consisting of 100 m*M* trisodium citrate–HCl buffer pH 5.6 containing 1.6–1.7 *M* ammonium sulfate and 200 m*M* potassium sodium tartrate (Fig. 1*c*). An ∼100 µm crystal of Lys-methylated SerRS^{Set2}–tRNA^{Sec} complex diffracted to 4.6 Å resolution and belonged to space group *I*432, with unit-cell parameters $a = b = c = 274.4$ Å (Table 1). The diffraction resolution was improved remarkably by introduction of the Tyr residues and was accompanied by expansion of the unit-cell length.

3.4. Improvement by point mutations (second trial)

An ∼100 µm crystal of Lys-methylated SerRS^{Set2}–tRNA^{Sec} complex was soaked in 10 m*M* $HgCl_2$ and diffraction data were collected at the peak X-ray wavelength of mercury. The crystal diffracted to 4.7 Å resolution and belonged to space group *I*432, with unit-cell parameters $a = b = c = 274.7$ Å (Table 1). SIRAS phasing was performed using diffraction data from the native and mercury-labelled crystals of the Lys-methylated SerRS^{Set2}–tRNA^{Sec} complex. Based on the updated $|F_o|$ map, Tyr and Arg residues were introduced into the SerRS surface involved in the protein–RNA contact of the crystal packing. The six-site point mutation E189R/D193R/E379Y/E383R/E497Y/E499Y was introduced into SerRS^{Set2} to create SerRS with 11 point-mutation sites (SerRS^{Set3}).

The Lys-methylated SerRS^{Set3}–tRNA^{Sec} complex was crystallized using a reservoir solution consisting of 100 m*M* trisodium citrate–HCl buffer pH 5.6 containing 1.3 *M* ammonium sulfate, 210 m*M* potassium sodium tartrate and 50 m*M* imidazole. However, the growth rate was extremely slow and the crystals were too small. In order to obtain larger crystals, the volume of the crystallization drop was increased (from 1.5 to 13.2 µl) and the number of crystal nuclei was controlled by seeding 20–50 µm crystals. The crystals grew to 500–800 µm in 6–8 weeks (Fig. 1*d*). They diffracted to ∼4.0 Å resolution and belonged to space group *I*432, with unit-cell parameters $a = b = c = 274$ Å (Table 1). Crystallization of the Lys-methylated SerRS^{Set3}–tRNA^{Sec} complex using SeMet-substituted SerRS^{Set3} was also performed in the same manner as for the native protein complex (Fig. 1*e*). An ∼500 µm crystal of the complex diffracted to ∼4.0 Å resolution and belonged to space group *I*432, with unit-cell parameters $a = b = c = 274$ Å. The improvement in the diffraction resolution was likely to be a consequence of the larger crystal sizes; the contributions of the additional point mutations were unclear.

3.5. Improvement by soaking in a heavy-atom reagent

To reinforce the phase information, heavy-atom labelling was examined by soaking crystals of the Lys-methylated SerRS^{Set3}–tRNA^{Sec} complex in 20 m*M* $HgCl_2$, K_2PtCl_4 or $K_2Pt(CN)_4$. The $HgCl_2$-soaked and the K_2PtCl_4-soaked crystals diffracted to 4.0 and 5.5 Å resolution, respectively. The heavy-atom labelling was monitored by XAFS measurements. In contrast, $K_2Pt(CN)_4$-soaked crystals diffracted to ∼3.2 Å resolution and belonged to space group *I*432, with unit-cell parameters $a = b = c = 273$ Å. Small cracks appeared in the crystals when they were transferred into the $K_2Pt(CN)_4$ solution, but the cracks became invisible during incubation. Therefore, $K_2Pt(CN)_4$ soaking may trigger slight slippage at the packing interface which results in an unexpected improvement of the diffraction resolution.

Diffraction data were collected from the $K_2Pt(CN)_4$-soaked crystal at three wavelengths (peak, edge and remote). 11 Pt-atom sites were identified based on the anomalous difference Fourier map generated using phases calculated from the preliminary models of SerRS and tRNA^{Sec}. The refined experimental phase was calculated using the MAD method (Table 1). In contrast, the highest resolution data (3.10 Å) were obtained from an SeMet-substituted crystal soaked with $K_2Pt(CN)_4$ (Table 1).

4. Discussion

M. kandleri SerRS contains 24 Lys residues (4.55%) and its theoretical isoelectric point is 4.9. The Lys methylation examined in this study did not alter the crystallization conditions and had either a neutral or a slightly negative effect on the diffraction resolution. However, it exerted a positive effect on crystal formation and growth.

Introducing point mutations in the protein–protein interface in the crystal packing had a negative effect on crystal formation and growth, and no crystals were obtained when SerRS^{Set1} was used. However, a dramatic improvement in the diffraction resolution was observed using SerRS^{Set2}. This indicated that the introduction of Tyr residues into the protein–protein interface could improve the diffraction resolution. In contrast, point mutations targeted to the protein–RNA interface had little effect on the resolution. Heavy-atom labelling can also affect the diffraction resolution. $K_2Pt(CN)_4$ soaking exhibited a positive effect, while neutral and negative effects were observed on $HgCl_2$ and K_2PtCl_4 soaking, respectively.

We thank the staff of SPring-8 BL41XU (Harima, Japan) and the Photon Factory beamlines (Tsukuba, Japan) for assistance with data collection. We also thank A. Ishii and T. Nakayama for assistance in manuscript preparation. This work was supported in part by Japan Society for the Promotion of Science (JSPS) Grants-in-Aid for Scientific Research (A) to SY and (C) to SS, the JSPS Global Centers of Excellence Program (Integrative Life Science Based on the Study of Biosignaling Mechanisms) and the Targeted Proteins Research Program of the Ministry of Education, Culture, Sports, Science and Technology. YI was supported by Research Fellowships from JSPS.

References

Baron, C., Westhof, E., Böck, A. & Giegé, R. (1993). *J. Mol. Biol.* **231**, 274–292.
Bilokapic, S., Maier, T., Ahel, D., Gruic Sovulj, I., Söll, D., Weygand-Durasevic, I. & Ban, N. (2006). *EMBO J.* **25**, 2498–2509.
Biou, V., Yaremchuk, A., Tukalo, M. & Cusack, S. (1994). *Science*, **263**, 1404–1410.
Böck, A., Forchhammer, K., Heider, J., Leinfelder, W., Sawers, G., Veprek, B. & Zinoni, F. (1991). *Mol. Microbiol.* **5**, 515–520.

Chiba, S., Itoh, Y., Sekine, S. & Yokoyama, S. (2010). *Mol. Cell*, **39**, 410–420.
Itoh, Y., Chiba, S., Sekine, S. & Yokoyama, S. (2009). *Nucleic Acids Res.* **37**, 6259–6268.
Jühling, F., Mörl, M., Hartmann, R. K., Sprinzl, M., Stadler, P. F. & Pütz, J. (2009). *Nucleic Acids Res.* **37**, D159–D162.
Leinfelder, W., Zehelein, E., Mandrand-Berthelot, M. A. & Böck, A. (1988). *Nature (London)*, **331**, 723–725.
McCoy, A. J., Grosse-Kunstleve, R. W., Adams, P. D., Winn, M. D., Storoni, L. C. & Read, R. J. (2007). *J. Appl. Cryst.* **40**, 658–674.
Otwinowski, Z. & Minor, W. (1997). *Methods Enzymol.* **276**, 307–326.
Sekine, S., Nureki, O., Sakamoto, K., Niimi, T., Tateno, M., Go, M., Kohno, T., Brisson, A., Lapointe, J. & Yokoyama, S. (1996). *J. Mol. Biol.* **256**, 685–700.
Sturchler, C., Westhof, E., Carbon, P. & Krol, A. (1993). *Nucleic Acids Res.* **21**, 1073–1079.
Vonrhein, C., Blanc, E., Roversi, P. & Bricogne, G. (2007). *Methods Mol. Biol.* **364**, 215–230.
Walter, T. S., Meier, C., Assenberg, R., Au, K. F., Ren, J., Verma, A., Nettleship, J. E., Owens, R. J., Stuart, D. I. & Grimes, J. M. (2006). *Structure*, **14**, 1617–1622.
Winn, M. D. *et al.* (2011). *Acta Cryst.* D**67**, 235–242.